

**R&D OF A HIGH-PERFORMANCE DIRC DETECTOR FOR
USE IN AN ELECTRON-ION COLLIDER**

by

S. Lee Allison
MS in Physics

A Dissertation Submitted to the Faculty of
Old Dominion University in Partial Fulfillment of the
Requirements for the Degree of

DOCTOR OF PHILOSOPHY

PHYSICS

OLD DOMINION UNIVERSITY
May 2017

Approved by:

Dr. Charles Hyde (Director)

Dr. Grzegorz Kalicy (Member)

member (Member)

ABSTRACT

R&D OF A HIGH-PERFORMANCE DIRC DETECTOR FOR USE IN AN ELECTRON-ION COLLIDER

S. Lee Allison
Old Dominion University, 2016
Director: Dr. Dr. Charles Hyde

text of abstract goes here

Copyright, 2016, by S. Lee Allison, All Rights Reserved.

ACKNOWLEDGEMENTS

Contents

LIST OF TABLES	vii
LIST OF FIGURES	viii
Chapter	
1. INTRODUCTION	2
2. ELECTRON-ION COLLIDER	3
2.1 SCIENCE GOALS	4
2.2 FACILITIES	6
3. DIRC TECHNOLOGY	10
3.1 CHERENKOV RADIATION	10
3.2 APPLYING THE CHERENKOV EFFECT TO PARTICLE ID	11
3.3 RING IMAGING DETECTORS	12
3.4 DIRC DETECTORS	12
4. HIGH-PERFORMANCE DIRC@EIC	15
4.1 EVOLUTION OF THE DIRC@EIC DESIGN	15
4.2 CURRENT HIGH-PERFORMANCE DIRC DESIGN	15
4.3 SIMULATED PERFORMANCE	15
4.4 POTENTIAL OPTIMIZATIONS	15
5. TEST BENCH EVALUATION OF DIRC@EIC COMPONENTS	16
5.1 OPTICAL PROPERTIES OF 3-LAYER LENS	16
5.2 RADIATION HARDNESS OF NLAK33 MATERIAL	16
5.3 PERFORMANCE OF PHOTOSENSORS IN HIGH MAGNETIC FIELD	16
6. 3-LAYER LENS PERFORMANCE IN PARTICLE BEAM	17
6.1 PROTOTYPE SETUP	17
6.2 SIMULATED PERFORMANCE	17
6.3 DATA ANALYSIS	17
7. OUTLOOK AND SUMMARY	18

BIBLIOGRAPHY	18
APPENDICES	
A. ERROR EVALUATION	20
VITA	21

List of Tables

List of Figures

2.1. The reduced cross section $\sigma_r(x, Q^2)$ as a function of Q^2 . Filled circles are combined H1 and Zeus data from HERA for proton-positron collisions, hollow squares are from fixed target experiments, and the yellow is prediction from HERAPDF0.1 (?)	4
2.2. Evolution of our understanding of nucleon spin structure. Left: In the 1980s, a nucleons spin was naively explained by the alignment of the spins of its constituent quarks. Right: In the current picture, valence quarks, sea quarks and gluons, and their possible orbital motion are expected to contribute to overall nucleon spin.	5
2.3. Ratio of the nucleon structure functions for Carbon and Deuterium for x between 0.2 and 0.9 and a range of Q^2 values.	6
2.4. Current design of the EIC facility for JLab with the two interaction points highlighted in red.	7
2.5. Current design of the EIC facility for BNL.	8
2.6. Current design of the detector to be used in the JLab EIC at IP1	9
3.1. Illustration of the Cherenkov cone.	11
3.2. Particle momentum versus Cherenkov angle for different particle species in fused silica ($n \approx 1.473$).	12
3.3. Schematic of a Proximity Focusing Ring Imaging Cherenkov (RICH) detector.	13
3.4. Annulus ring of RICH detector.	14
3.5. The basic components of a DIRC detector: a solid radiator, typically fused silica (green); a mirror to redirect backward-going photons (pink); optional focusing optics (purple); an expansion volume to allow photons to separate in space (cyan); and a detector surface to record the position and arrival time of Cherenkov photons (maroon).	14

Comments

grab some papers from EMC collaboration and JLAB for references	5
I feel like I should say more about eRHIC here since I said so much about JLEIC	7

CHAPTER 1

INTRODUCTION

CHAPTER 2

ELECTRON-ION COLLIDER

It has been known for nearly a century that atoms are composed of nucleons (protons and neutrons), but it took another 50 years for Murray Gell-Mann and George Zweig to independently develop a model proposing that nucleons themselves are made up of constituent components, called quarks, bound together by the exchange of gluons [1]. This lead to the development of the fundamental theory of the strong interaction, known as Quantum Chromo-Dynamics (QCD). It is now a strong goal of the nuclear physics community to understand the interactions of quarks and gluons and how those interactions make manifest both nucleons themselves, which account for nearly all the mass of the visible matter in the universe, as well as the nucleons' spin, mass, magnetic moment, and nuclear binding energy. Because of the well-known properties of the electromagnetic interaction, electron scattering is an ideal process for such studies.

Although it would theoretically be possible to study these properties using fixed-target electron beam experiments, it is three-fold prohibitive: it is much more costly to construct an accelerator to accelerate electrons to the necessary momentum (on the order of TeV) than to build a collider, it is more difficult and complicated to do transverse nucleon polarization studies with a fixed target due to the nature of the required magnetic fields, and it is very difficult to study the target fragments of a fixed target reactions due to final state interactions whereas in a collider the fragments will be boosted in the same direction as the ion beam. It was therefore deemed a priority by the 2007 Nuclear Science Advisory Committee's Long-Range Plan that an Electron-Ion Collider (EIC) be the next facility to be built in the United States [2].

The EIC will not be the first facility to have the capability of colliding electrons and positrons with protons. The HERA accelerator in Hamburg, Germany was the world's first electron-proton collider, reaching electron energies of up to 28 GeV and protons to nearly 1 TeV with a luminosity on the order of $10^{31} \text{ cm}^{-2} \text{ s}^{-1}$ before shutting down in 2007. Figure ?? shows the combined H1 and Zeus experimental data from HERA for the measurement of the structure function for positron-proton scattering along with fixed target data for a wide range of both x and Q^2 . The EIC hopes to improve upon the already rich science produced at HERA threefold: by increasing the luminosity of the accelerator to on the

order of $10^{34} \text{ cm}^{-2} \text{ s}^{-1}$, by allowing for the use of heavier ion beams such as oxygen, and by allowing for both transversely and longitudinally polarized beams of electrons and light ions. With these improvements the EIC will be able to look into hadronic final states with much greater detail.

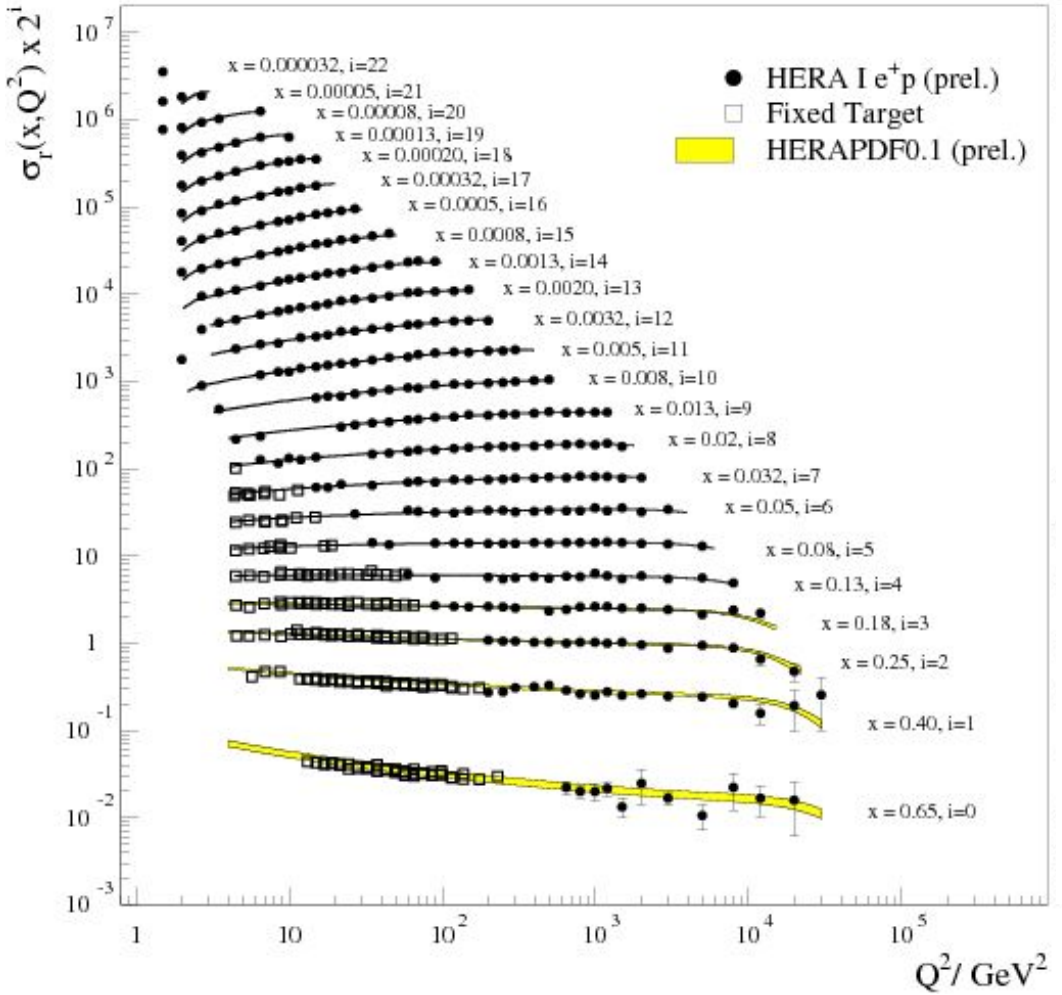


FIG. 2.1: The reduced cross section $\sigma_r(x, Q^2)$ as a function of Q^2 . Filled circles are combined H1 and Zeus data from HERA for proton-positron collisions, hollow squares are from fixed target experiments, and the yellow is prediction from HERAPDF0.1 (?)

2.1 SCIENCE GOALS

The goal of an EIC will be to find out how QCD is responsible for the structure and dynamics of nucleons, the nature of the nucleon-nucleon force, and the relative importance of the valance quarks.

2.1.1 NUCLEON SPIN

One major question still pestering nuclear physicists is “What is the origin of the nucleon spin?”. In the 1980s the naive answer was that the total nucleon spin was the sum of the spin of its three valence quarks, but many years of experimentation has revealed that it is much more complicated (Fig. 2.2), with the contributions from gluons and orbital angular momentum still in question. The EIC will be capable of much more detailed study of the contributions to the nucleon structure by enabling multi-dimensional projections of the distribution of quarks and gluons in space, longitudinal and transverse momenta, spin, and flavor.

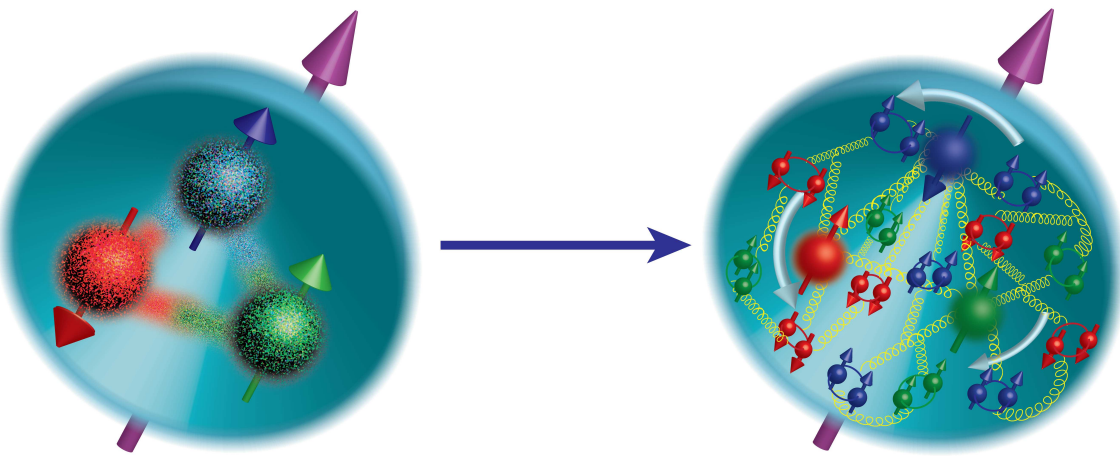


FIG. 2.2: Evolution of our understanding of nucleon spin structure. **Left:** In the 1980s, a nucleon's spin was naively explained by the alignment of the spins of its constituent quarks. **Right:** In the current picture, valence quarks, sea quarks and gluons, and their possible orbital motion are expected to contribute to overall nucleon spin.

2.1.2 THE EMC EFFECT

It was first observed by the European Muon Collaboration (EMC), and confirmed by other experiments **grab some papers from EMC collaboration and JLAB for references** that there is a modification between the nucleon structure function, F_2 , of deuterium to those of heavier elements as a function of Bjorken x . Figure 2.3 shows the ratio of structure functions of Carbon and Deuterium for x between 0.2 and 0.9. Initial assumptions were that this ratio of structure functions would be unity, but measurements have clearly shown a suppression in this ratio for x values between 0.3 and 0.8.

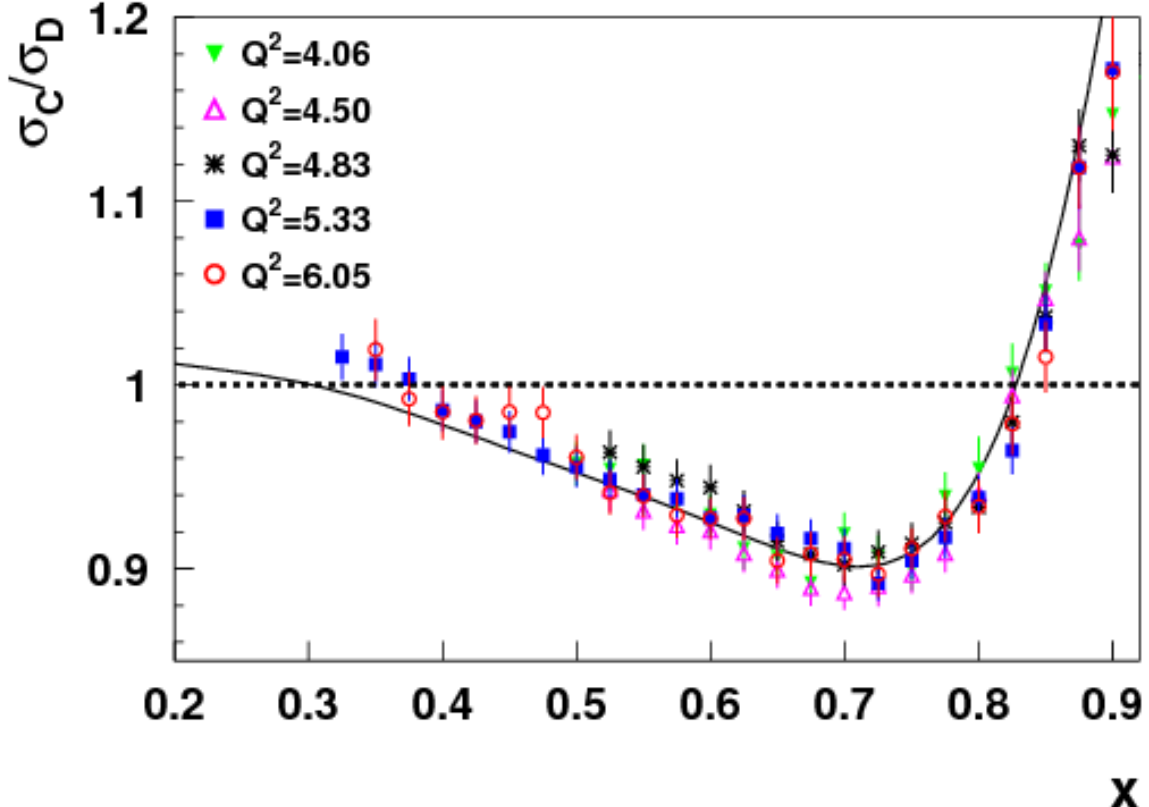


FIG. 2.3: Ratio of the nucleon structure functions for Carbon and Deuterium for x between 0.2 and 0.9 and a range of Q^2 values.

The reason for this modification to the nuclear structure function is still a mystery, but the EIC hopes to shed light on this phenomenon by studying various coherent exclusive reactions, such as J/Ψ production, which could allow for the quantification of initial conditions in heavy-ion collisions by mapping out the geometry of the nucleus in high-energy processes. This mapping can also help to understand other collective dynamics, such as shadowing and anti-shadowing.

2.1.3 GLUON DISTRIBUTIONS INSIDE NUCLEI

As mentioned above, the EMC effect, the modification of the distribution of quarks in a nucleus versus their distribution in nucleons, is a known (yet still mysterious) phenomenon. It is still unknown whether the same holds true for gluons. The EIC hopes to measure this suppression of the structure functions thanks to its wider range of kinematics both in x and Q^2 , being able to reach much lower x values and approach the region of gluon saturation.

2.2 FACILITIES

As of the writing of this thesis there are two competing designs for an EIC facility to be built in the United States: a figure-8 accelerator design for Thomas Jefferson National Accelerator Facility (JLab) (Figure 2.4), and a ring-ring accelerator design for Brookhaven National Lab (BNL) (Figure 2.5).

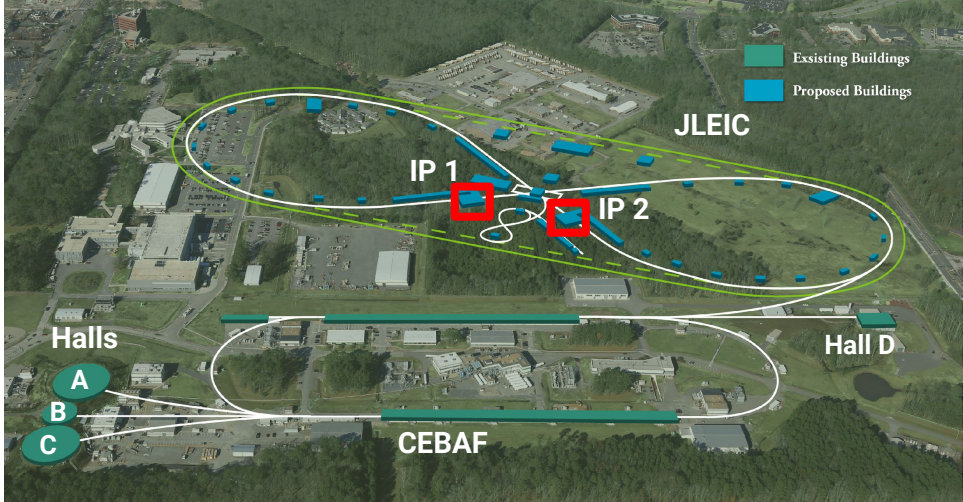


FIG. 2.4: Current design of the EIC facility for JLab with the two interaction points highlighted in red.

The JLab EIC (JLEIC) is planned to be approximately 1.4 km in circumference and have a footprint of roughly 500 m by 170 m. The design is a ring-ring with electrons and ions being stored in separate beam lines and collided at two interaction points (IPs) (outlined in red in Figure 2.4) on the figure-8. The JLab CEBAF SRF linac will be used as an electron injector for electrons with 3 - 11 GeV energy. The second ring will store an ion beam with energy of 20 to 100 GeV for protons or up to 40 GeV per nucleon for light to heavy ions. The ion beams are generated and accelerated in a new ion injector complex with the same figure-8 design that will be utilized to preserve ion polarization. The two rings will be stacked vertically in the same underground tunnel [3].

The BNL facility, named eRHIC, will use a new electron beam facility based on an Energy Recovery LINAC that will be built inside of the Relativistic Heavy Ion Collider (RHIC) tunnel to collide with RHIC's pre-existing polarized proton/ion beam (Fig. 2.5). **I feel like I should say more about eRHIC here since I said so much about JLEIC**

2.2.1 JLEIC DETECTOR DESIGN

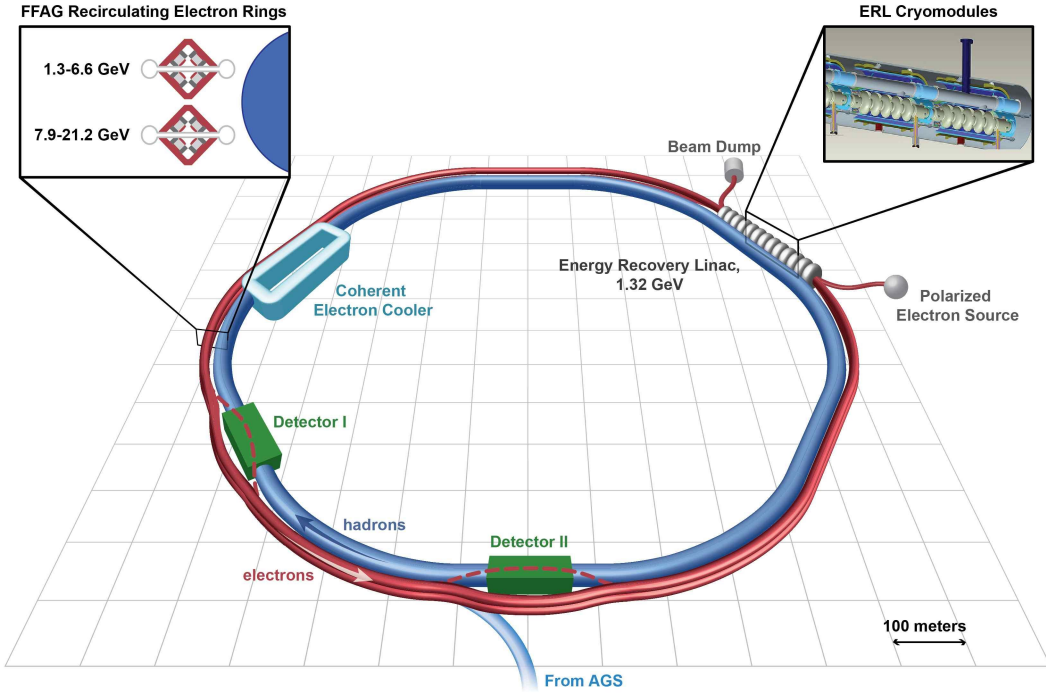


FIG. 2.5: Current design of the EIC facility for BNL.

The large center of mass energies and diverse physics program at an EIC necessitate a very sophisticated detector system. Figure 2.6 shows the current design of the JLab EIC detector at IP1. This

2.2.2 PARTICLE IDENTIFICATION

The ability to accurately identify hadrons in the final state is a key requirement for the physics program at an EIC.

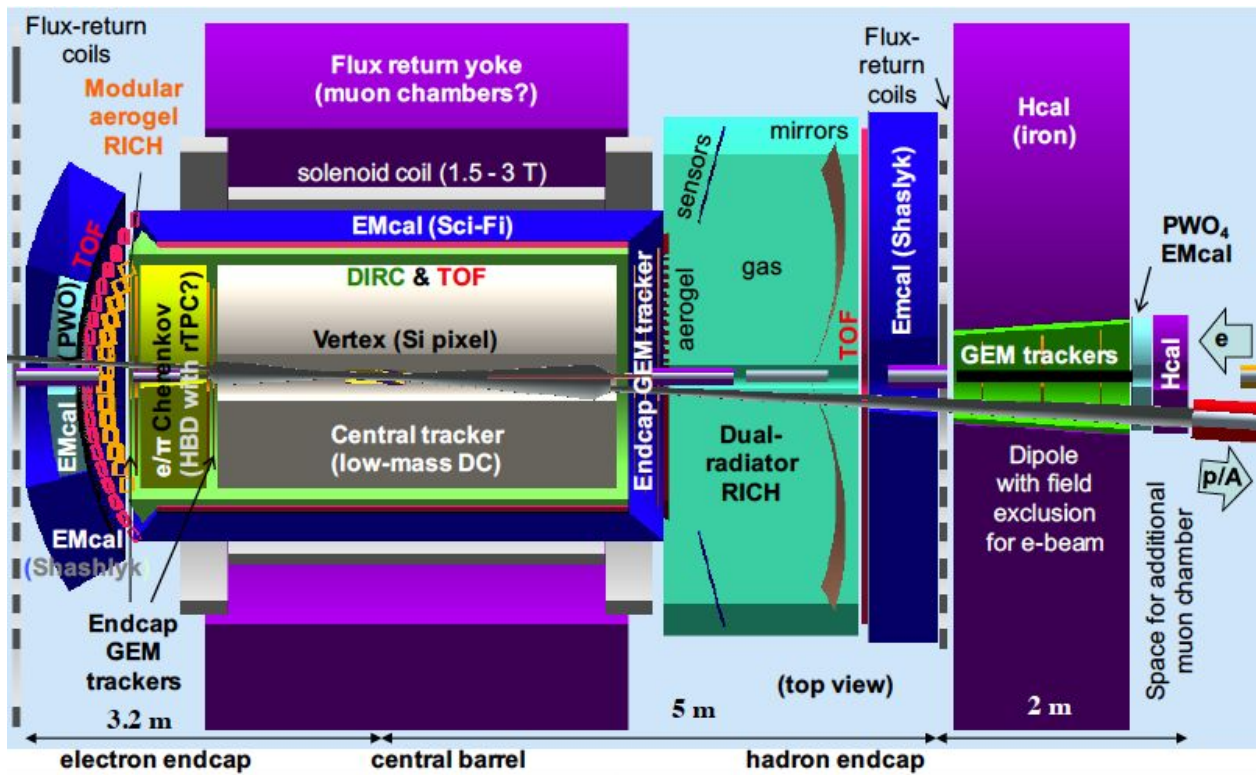


FIG. 2.6: Current design of the detector to be used in the JLab EIC at IP1

CHAPTER 3

DIRC TECHNOLOGY

The DIRC detector is based on the concept of the Detection of Internally Reflected Cherenkov light (DIRC) produced in a solid radiator bar to identify charged particle. It is a special type of Cherenkov counter, which uses the unique properties of Cherenkov radiation.

3.1 CHERENKOV RADIATION

Einstein postulated in his Theory of Relativity that the speed of light in a vacuum, c , is the limit of the velocity of massive particles. In an optically transparent medium, however, the speed at which light propagates is modified: $c_{med} = c/n$, where n is the index of refraction of the medium. Pavel Cherenkov discovered in 1934 that massive particles moving through a medium faster than the speed of light in that medium emit light in the form of now-called Cherenkov radiation. Cherenkov was able to establish several interesting properties of this radiation: it is only emitted from charged particles above a certain velocity threshold $v > c/n$, the intensity is proportional to the particle's path length, emission is prompt, and the light is polarized with a continuous wavelength spectrum. Later in 1937 Ilya Frank and Igor Tamm theoretically formulated this radiation with fantastic agreement to Cherenkov's findings, and the three shared the 1958 Nobel Prize in Physics for their efforts [?].

Further studies confirmed that Cherenkov radiation is emitted uniformly in azimuth (ϕ_c) around the particle's direction of travel with the polar opening angle θ_C defined as

$$\cos \theta_C = \frac{1}{\beta n(\lambda)}, \quad (3.1)$$

where $\beta = v_p/c$, v_p is the particle's velocity, and the index of refraction is a function of the emitted photon wavelength. In a normal, dispersive optical medium the opening half-angle of the shock wave produced by the Cherenkov radiation, η_C defined in Figure 3.1, is not complementary to the Cherenkov angle. The relationship between the two is given by

$$\cot \eta_C = \left[\frac{d}{d\omega} (\omega \tan \theta_C) \right]_{\omega_0} = \left[\tan \theta_C + \beta^2 \omega n(\omega) \frac{dn}{d\omega} \cot \theta_C \right]_{\omega_0} \quad (3.2)$$

where ω_0 is the central value of the considered frequency range. Because the second term in (3.2) is zero only for non-dispersive media the shock wave front is not perpendicular to the Cherenkov cone in real detectors.

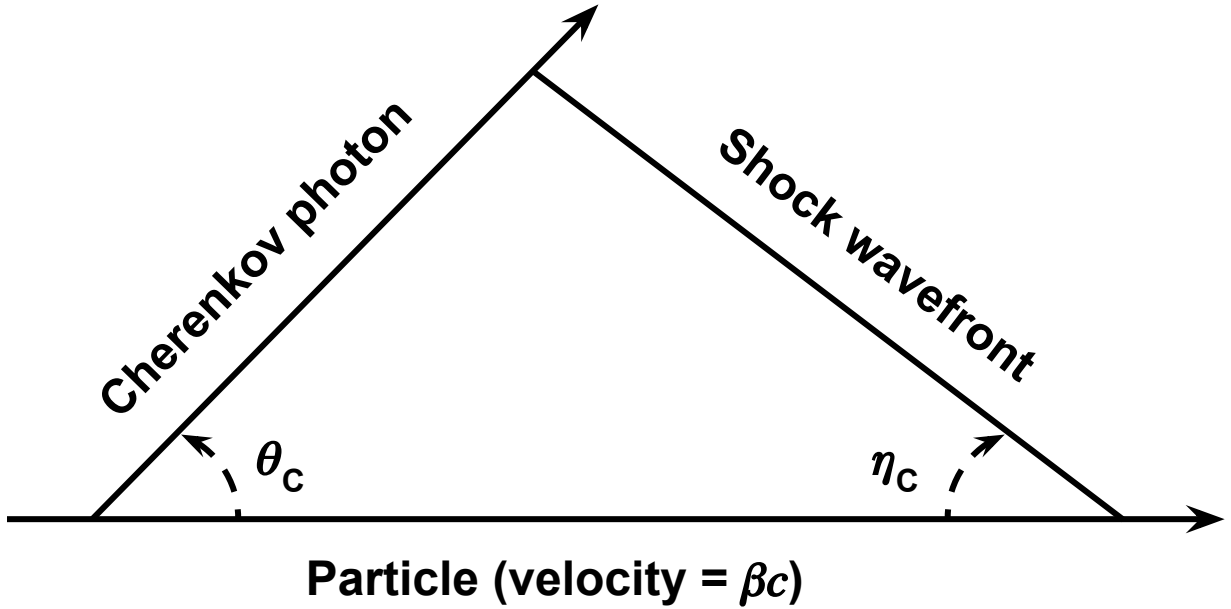


FIG. 3.1: Illustration of the Cherenkov cone.

Because particles lose very little energy when radiating Cherenkov photons the emission is very weak. The number of photons $N_{photons}$ emitted per path length L (in cm) by a moving particle with charge z is given by the Frank-Tamm equation

$$\frac{N_{photons}}{L} = \frac{\alpha^2 z^2}{r_e m_e c^2} \int \sin^2 \theta_C(E) dE \quad (3.3)$$

where E is the photon energy in eV, the integral is taken over the region where $n(E)$ is greater than 1, and $\frac{\alpha^2 z^2}{r_e m_e c^2} = 370 \text{ cm}^{-1} \text{ eV}^{-1}$.

3.2 APPLYING THE CHERENKOV EFFECT TO PARTICLE ID

In order to identify particle species one must know both the mass and charge of the particle in question. Because the Cherenkov angle encodes the particle's velocity it is, in principle, a simple matter to measure the particle's momentum with a tracking chamber as well as the velocity obtained from (3.1) to determine the mass and charge. Figure 3.2 shows how different particle species can be distinguished for a given momentum in fused silica.

Threshold Cherenkov counters are detectors used for particle identification (PID) by exploiting the fact that only particles above the threshold velocity $\beta > 1/n$ will emit Cherenkov

photons. The information about a particle's velocity can be combined with momentum information from a tracking system to determine the mass as [?]

$$m = \frac{p}{c} \sqrt{n^2 \cos^2 \theta_C - 1} \quad (3.4)$$

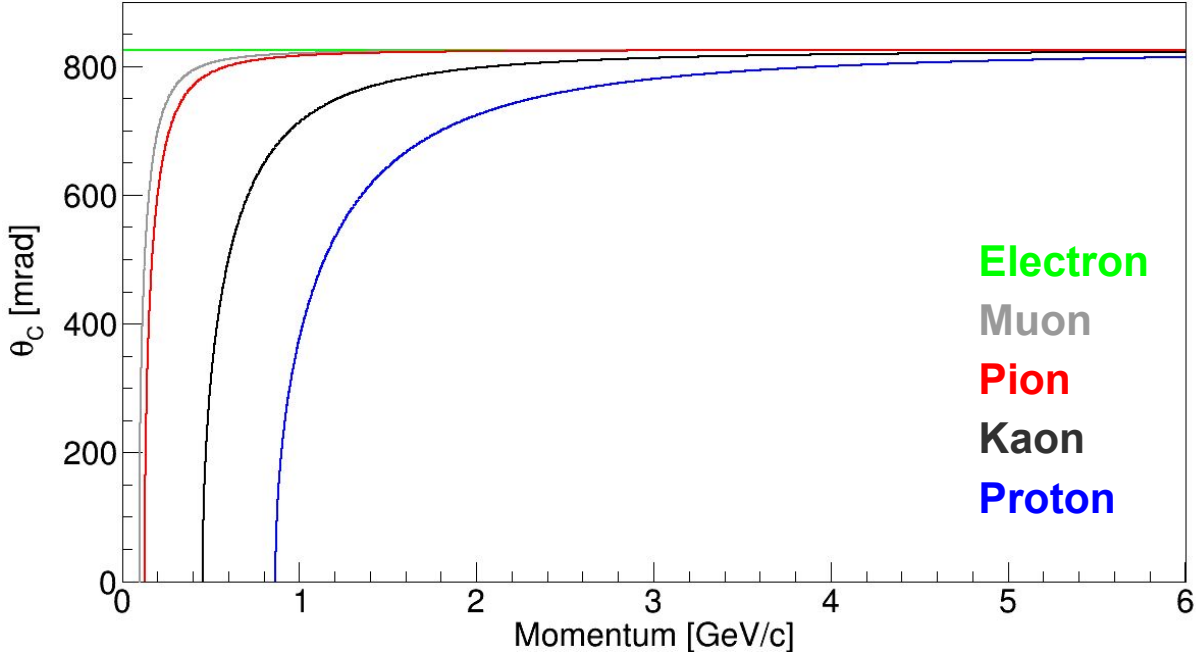


FIG. 3.2: Particle momentum versus Cherenkov angle for different particle species in fused silica ($n \approx 1.473$).

3.3 RING IMAGING DETECTORS

Ring Imaging Cherenkov (RICH) detectors are designed to efficiently identify and separate different particle species over a wide range of momenta. A basic RICH system is shown in Figure 3.3.

A volume of radiator, either gaseous (e.g. C_4F_{10}) or solid (e.g. aerogel), is positioned upstream of an array of photosensors. A charged particle travelling through a thin radiator above the threshold velocity will continuously emit Cherenkov photons in a cone. The resulting image on the photosensor array is an annulus of thickness $L \tan \theta_C$, where L is the distance the particle travelled inside the radiator, and θ_C is the usual Cherenkov angle (Figure 3.4). PID can be done by measuring the average radius of the annulus and reconstructing the Cherenkov angle geometrically.

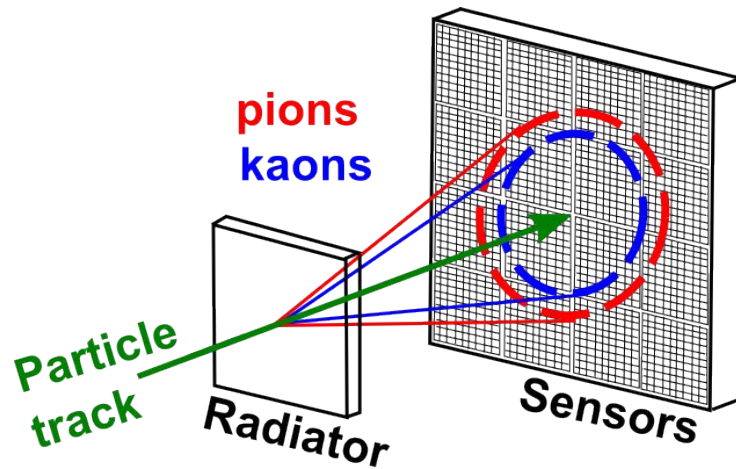


FIG. 3.3: Schematic of a Proximity Focusing Ring Imaging Cherenkov (RICH) detector.

3.4 DIRC DETECTORS

The basic components of a DIRC detector are shown in Figure 3.5.

3.4.1 DIRCS IN FUTURE EXPERIMENTS

EIC, PANDA, Bell, ToRCH, GlueX

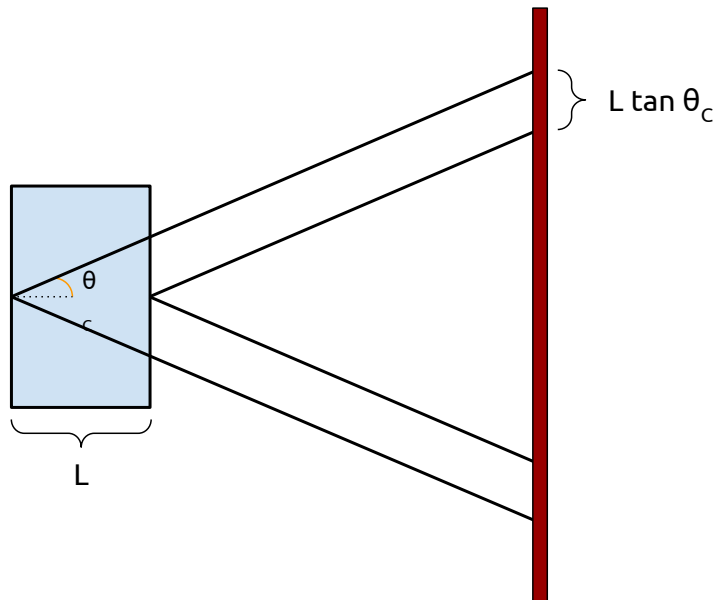


FIG. 3.4: Annulus ring of RICH detector.

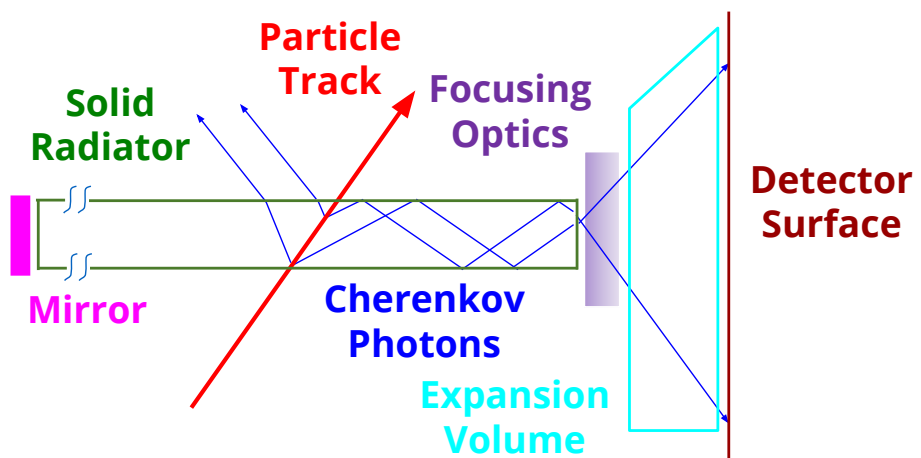


FIG. 3.5: The basic components of a DIRC detector: a solid radiator, typically fused silica (green); a mirror to redirect backward-going photons (pink); optional focusing optics (purple); an expansion volume to allow photons to separate in space (cyan); and a detector surface to record the position and arrival time of Cherenkov photons (maroon).

CHAPTER 4

HIGH-PERFORMANCE DIRC@EIC

4.1 EVOLUTION OF THE DIRC@EIC DESIGN

4.2 CURRENT HIGH-PERFORMANCE DIRC DESIGN

4.3 SIMULATED PERFORMANCE

4.4 POTENTIAL OPTIMIZATIONS

CHAPTER 5

TEST BENCH EVALUATION OF DIRC@EIC COMPONENTS

5.1 OPTICAL PROPERTIES OF 3-LAYER LENS

5.2 RADIATION HARDNESS OF NLAK33 MATERIAL

5.3 PERFORMANCE OF PHOTOSENSORS IN HIGH MAGNETIC
FIELD

CHAPTER 6

3-LAYER LENS PERFORMANCE IN PARTICLE BEAM

6.1 PROTOTYPE SETUP

6.2 SIMULATED PERFORMANCE

6.3 DATA ANALYSIS

6.3.1 ERROR EVALUATION

CHAPTER 7

OUTLOOK AND SUMMARY

BIBLIOGRAPHY

- [1] Bill Carithers and Paul Grannis. Discovery of the top quark. *Beam Line*, 25(3):4–16, 1995.
- [2] Robert Tribble et. al. *Frontiers of Nuclear Science*. 2007.
- [3] S. Abeyratne et al. MEIC Design Summary. 2015.

APPENDIX A

ERROR EVALUATION

VITA

S. Lee Allison
Department of Physics
Old Dominion University
Norfolk, VA 23529

The text of the Vita goes here.